LETTERS

Stream denitrification across biomes and its response to anthropogenic nitrate loading

Patrick J. Mulholland[1,2], Ashley M. Helton[3], Geoffrey C. Poole[3,4], Robert O. Hall Jr[5], Stephen K. Hamilton[6], Bruce J. Peterson[7], Jennifer L. Tank[8], Linda R. Ashkenas[9], Lee W. Cooper[2], Clifford N. Dahm[10], Walter K. Dodds[11], Stuart E. G. Findlay[12], Stanley V. Gregory[9], Nancy B. Grimm[13], Sherri L. Johnson[14], William H. McDowell[15], Judy L. Meyer[3], H. Maurice Valett[16], Jackson R. Webster[16], Clay P. Arango[8], Jake J. Beaulieu[8]†, Melody J. Bernot[17], Amy J. Burgin[6], Chelsea L. Crenshaw[10], Laura T. Johnson[8], B. R. Niederlehner[16], Jonathan M. O'Brien[6], Jody D. Potter[15], Richard W. Sheibley[13]†, Daniel J. Sobota[9]† & Suzanne M. Thomas[7]

Anthropogenic addition of bioavailable nitrogen to the biosphere is increasing[1,2] and terrestrial ecosystems are becoming increasingly nitrogen-saturated[3], causing more bioavailable nitrogen to enter groundwater and surface waters[4–6]. Large-scale nitrogen budgets show that an average of about 20–25 per cent of the nitrogen added to the biosphere is exported from rivers to the ocean or inland basins[7,8], indicating that substantial sinks for nitrogen must exist in the landscape[9]. Streams and rivers may themselves be important sinks for bioavailable nitrogen owing to their hydrological connections with terrestrial systems, high rates of biological activity, and streambed sediment environments that favour microbial denitrification[6,10,11]. Here we present data from nitrogen stable isotope tracer experiments across 72 streams and 8 regions representing several biomes. We show that total biotic uptake and denitrification of nitrate increase with stream nitrate concentration, but that the efficiency of biotic uptake and denitrification declines as concentration increases, reducing the proportion of in-stream nitrate that is removed from transport. Our data suggest that the total uptake of nitrate is related to ecosystem photosynthesis and that denitrification is related to ecosystem respiration. In addition, we use a stream network model to demonstrate that excess nitrate in streams elicits a disproportionate increase in the fraction of nitrate that is exported to receiving waters and reduces the relative role of small versus large streams as nitrate sinks.

Biotic nitrogen uptake and denitrification account for nitrogen removal in streams, but a broad synthesis of their relative importance is lacking, in part because of the difficulty of measuring denitrification *in situ* and the lack of comparable data for streams across biomes and land-use conditions. The second Lotic Intersite Nitrogen Experiment (LINX II), a series of ^{15}N tracer additions to 72 streams across multiple biomes and land uses in the conterminous United States and Puerto Rico, provides replicated, *in situ* measurements of total nitrate (NO_3^-) uptake and denitrification. This new data set expands more than tenfold the number and type of streams for which we have reach-scale measurements of denitrification, the primary mechanism by which bioavailable nitrogen is permanently removed from ecosystems.

Streams were small (discharge: 0.2 to 268 l s^{-1}; median: 18.5 l s^{-1}) but spanned a wide range of NO_3^- concentration (0.0001 to 21.2 mg N l^{-1}; median: 0.10 mg N l^{-1}) and other environmental conditions such as water velocity, depth and temperature (Supplementary Table 1). Concentrations of NO_3^- were significantly greater in 'agricultural' and 'urban' streams than in 'reference' streams (Fig. 1a), despite substantial variation in the adjacent land use and in-stream conditions within each of these land-use categories.

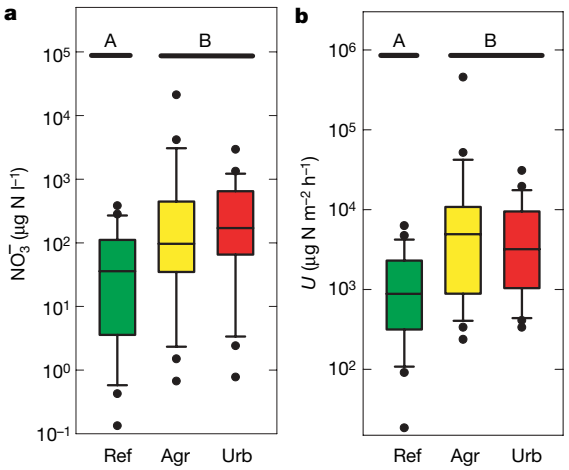

Figure 1 | Observed stream NO_3^- metrics by adjacent land use. **a**, Streamwater NO_3^- concentration. **b**, Total biotic NO_3^- uptake rate per unit area of streambed (U). Box plots display 10th, 25th, 50th, 75th and 90th percentiles, and individual data points outside the 10th and 90th percentiles. Land use had a significant effect on NO_3^- concentration ($P = 0.0055$) and U ($P = 0.0013$) (Kruskal–Wallis test); horizontal bars above plots denote significant differences determined by pairwise comparisons among land-use categories with Bonferroni correction ($\alpha = 0.05$).

[1]Environmental Sciences Division, Oak Ridge National Laboratory, Oak Ridge, Tennessee 37831, USA. [2]Department of Ecology and Evolutionary Biology, University of Tennessee, Knoxville, Tennessee 37996, USA. [3]Odum School of Ecology, University of Georgia, Athens, Georgia 30602, USA. [4]Eco-metrics, Inc., Tucker, Georgia 30084, USA. [5]Department of Zoology and Physiology, University of Wyoming, Laramie, Wyoming 82071, USA. [6]Kellogg Biological Station, Michigan State University, Hickory Corners, Michigan 49060, USA. [7]Ecosystems Center, Marine Biological Laboratory, Woods Hole, Massachusetts 02543, USA. [8]Department of Biological Sciences, University of Notre Dame, Notre Dame, Indiana 46556, USA. [9]Department of Fisheries and Wildlife, Oregon State University, Corvallis, Oregon 97331, USA. [10]Department of Biology, University of New Mexico, Albuquerque, New Mexico 87131, USA. [11]Division of Biology, Kansas State University, Manhattan, Kansas 66506, USA. [12]Institute of Ecosystem Studies, Millbrook, New York 12545, USA. [13]School of Life Sciences, Arizona State University, Tempe, Arizona 85287, USA. [14]Pacific Northwest Research Station, US Forest Service, Corvallis, Oregon 97331, USA. [15]Department of Natural Resources, University of New Hampshire, Durham, New Hampshire 03824, USA. [16]Department of Biological Sciences, Virginia Tech, Blacksburg, Virginia 24061, USA. [17]Department of Biology, Ball State University, Muncie, Indiana 47306, USA. †Present addresses: US Environmental Protection Agency, Cincinnati, Ohio 45268, USA (J.J.B.); US Geological Survey, Tacoma, Washington 98402, USA (R.W.S.); School of Earth and Environmental Sciences, Washington State University, Vancouver Campus, Vancouver, Washington 98686, USA (D.J.S.).

Areal rate of total NO_3^- uptake (U, mass of NO_3^- removed from water per unit area of streambed per unit time) also was greater in agricultural and urban streams (Fig. 1b), suggesting that higher NO_3^- concentration stimulates uptake in these streams. Total uptake velocity of NO_3^- (v_f, analogous to the average downward velocity at which NO_3^- ions are removed from water, and a measure of uptake efficiency relative to availability[12]) was unrelated to land-use category but declined exponentially with increasing NO_3^- concentration (Fig. 2a). Thus, although excess NO_3^- increased uptake rate per area of streambed, streams became less efficient at removing NO_3^-, indicating that uptake does not increase in parallel with NO_3^- concentration. The value of v_f also increased with increasing gross primary production rate ($r^2 = 0.204$, $P < 0.0001$), revealing the importance of stream photoautotrophs in NO_3^- removal. Although other research has documented the separate influence of NO_3^- concentration[13,14] and gross primary production rate[15,16] on v_f within a particular biome, our data reveal their combined influence on NO_3^- removal efficiency, and demonstrate that the loss of efficiency holds across nearly six orders of magnitude in NO_3^- concentration and eight different regions representing several different biomes.

A portion of total NO_3^- uptake in streams can be attributed to denitrification, a microbial process occurring mostly in anoxic zones in the streambed that converts NO_3^- to gaseous forms of nitrogen that are lost to the atmosphere. Our ^{15}N-tracer approach allowed us to directly quantify uptake velocity resulting from denitrification of streamwater NO_3^- (v_{fden}). The remainder of total NO_3^- uptake represents biotic assimilation and storage in organic (usually particulate) form on the streambed. Some portion of stored nitrogen may be subsequently denitrified via tight spatial coupling of mineralization, nitrification and denitrification in sediments ('coupled denitrification'), which can be important in aquatic systems with NO_3^- concentrations below ~300 μg N l^{-1} (ref. 10). Thus, v_f describes the upper limit and v_{fden} the lower limit on rates of biotic NO_3^- removal from stream water.

Like v_f, v_{fden} declined exponentially as NO_3^- concentration increased (Fig. 2b), indicating reduced NO_3^- removal efficiency via denitrification with increasing NO_3^- concentration. It also increased with increasing ecosystem respiration rate ($r^2 = 0.318$, $P < 0.0001$), probably because aerobic respiration (that is, ecosystem respiration rate) lowers dissolved oxygen concentration and increases metabolic demand for alternative electron acceptors such as NO_3^-. In addition, ecosystem respiration is likely to be a good surrogate for the availability of labile organic carbon to fuel denitrification. The denitrification fraction of total NO_3^- uptake (ratio of v_{fden} to v_f) was highly variable across streams and was unrelated to land use (Fig. 3a), but was positively correlated with ecosystem respiration rate ($r = 0.40$, $P = 0.005$), further supporting the hypothesis that heterotrophic metabolism promotes denitrification[17].

Denitrification accounted for a median of 16% of total NO_3^- uptake across all streams, and exceeded 43% of total uptake in a quarter of our streams. These values are conservative, however, because our measurement method does not account for delayed, coupled denitrification that may occur after NO_3^- is assimilated by biota and remineralized in sediments[10].

Areal denitrification rate (U_{den}), a measure commonly reported in denitrification studies, was greatest in urban streams (Fig. 3b), probably because of high NO_3^- concentration (Fig. 1a). Although our measurements of U_{den} fall within the range observed for other aquatic systems[18], they are lower than other published values for rivers (Fig. 3b), possibly because they do not include coupled denitrification in sediments. However, our measurements of *in situ*, reach-scale denitrification may be more representative of stream ecosystem denitrification than the more commonly used acetylene-block technique in sediment cores[18].

In stream networks, any NO_3^- not removed within a reach passes to the next reach downstream, where it may be subsequently removed. Stream size influences this serial processing in several ways. Small streams can remove NO_3^- efficiently (because of their high ratios of streambed area to water volume) and have a cumulative influence on whole-network removal because they account for most of the stream length within a network[19,20]. By contrast, larger streams are effective NO_3^- sinks owing to longer transport distances and therefore longer water residence times combined with higher nitrogen availability[21,22].

We developed a stream network model of NO_3^- removal, incorporating downstream NO_3^- transport through streams of increasing size and using removal rates that varied with NO_3^- concentration

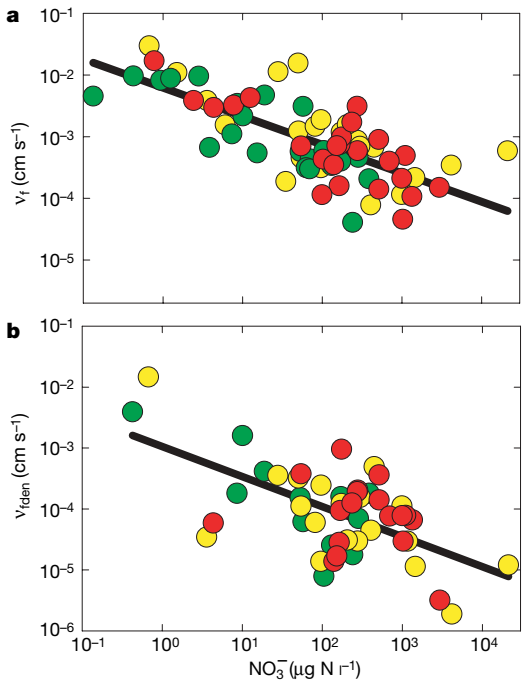

Figure 2 | Relationships between NO_3^- uptake velocity and concentration. **a**, Regression of total NO_3^- uptake velocity (v_f) on NO_3^- concentration (log $v_f = -0.462 \times \log[NO_3^-] - 2.206$, $r^2 = 0.532$, $P < 0.0001$). **b**, Regression of denitrification uptake velocity (v_{fden}) on NO_3^- concentration (log $v_{fden} = -0.493 \times \log[NO_3^-] - 2.975$, $r^2 = 0.355$, $P < 0.0001$).

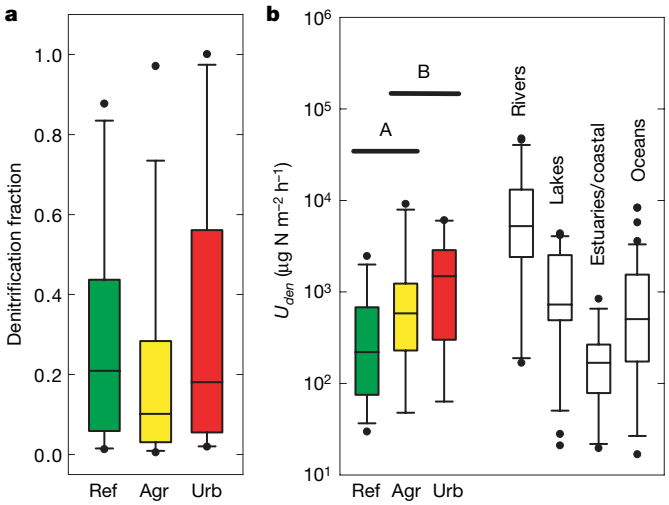

Figure 3 | Observed stream denitrification rates by adjacent land use. **a**, Denitrification as a fraction of total NO_3^- uptake. **b**, Denitrification rate per unit area of streambed (U_{den}), including denitrification rates in other aquatic ecosystems (uncoloured box plots) from a recent compilation[18]. Land use had a significant effect on U_{den} ($P = 0.049$) (Kruskal–Wallis test); horizontal bars above plots denote significant differences determined by pairwise comparisons among land-use categories with Bonferroni correction ($\alpha = 0.05$).

(Fig. 2). We used v_f and v_{fden}, respectively, to model the upper and lower limits on NO_3^- removal. Because our empirically derived rates of denitrification are apt to be conservative (for example, Fig. 3b), so too are the magnitudes of whole-network denitrification predicted by our model. Regardless, the model shows that NO_3^- loading rates may markedly influence the importance of streams as landscape nitrogen sinks. For instance, higher loading rates stimulate NO_3^- uptake and denitrification, but yield an associated disproportionate increase in downstream NO_3^- export to receiving waters (Fig. 4a) as

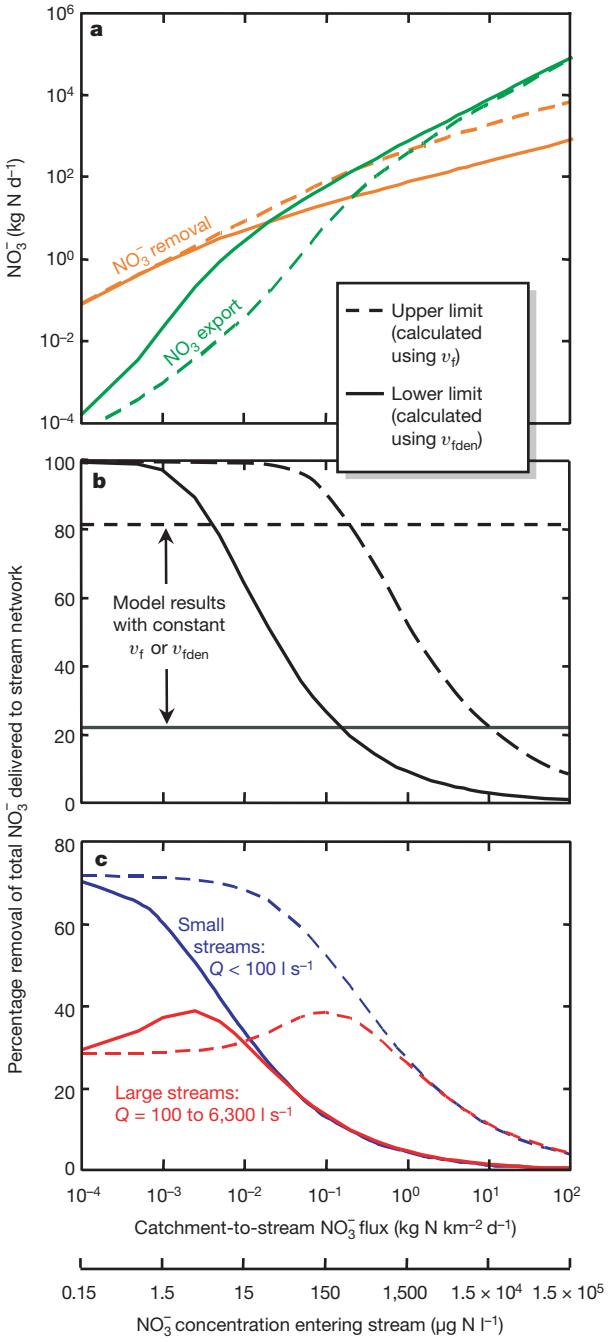

Figure 4 | Simulated upper and lower limits on biotic removal of NO_3^- from stream water within a fifth-order network. **a**, Removal and export of NO_3^- to receiving water bodies versus NO_3^- loading rate (and equivalent concentration in catchment water entering the stream). **b**, Biotic removal expressed as a percentage of total NO_3^- loading to the stream network versus NO_3^- loading rate; curves represent model results when v_f or v_{fden} varies with NO_3^- concentration (according to relationships in Fig. 2), horizontal lines show results using a constant v_f or v_{fden}. **c**, Same as curves in **b**, but divided among 'small' and 'large' streams.

NO_3^- removal efficiency declines (Fig. 4b). The loss of removal efficiency is not addressed by models where v_f is independent of NO_3^- concentration[22], which may yield overly optimistic projections of stream network NO_3^- removal under increasing loading rates (Fig. 4b).

Small and large streams responded differently to simulated increases in NO_3^- loading. The simulated percentage of network NO_3^- load removed in small streams declined as loading increased (Fig. 4c). Unexpectedly, in large streams, simulated percentage removal peaked after NO_3^- loading began to rise, owing to the interaction of two dynamics. Left of the peak, high removal efficiency in small streams yields little downstream NO_3^- transport from small to large streams (Fig. 4a), and therefore, little NO_3^- available for removal in large streams. Thus, percentage removal in large streams increases with NO_3^- loading as downstream transport of NO_3^- increases and large streams are released from NO_3^- limitation. Right of the peak, NO_3^- concentrations in large streams increase to the point where removal efficiency in large streams is lost, and the percentage removal in large streams decreases.

Our modelling results suggest three phases of nitrogen dynamics in stream networks as land-use intensity increases. First, at low nitrogen loading rates, biotic nitrogen removal is high and occurs primarily in smaller streams; removal in larger streams is limited by nitrogen availability. Second, at moderate loading rates, removal efficiency in smaller streams decreases; however, removal in larger streams responds, limiting nitrogen export. Third, at high loading rates, removal becomes ineffective across all stream sizes and the stream network exports virtually all catchment-derived nitrogen. Interestingly, direct anthropogenic NO_3^- loading to large streams (for example, municipal wastewater plants) circumvents the stream network, and therefore may increase the relative role of large versus small streams in network NO_3^- removal. Thus, both small and large streams can be important locations for nitrogen removal, although their relative roles are influenced by uptake efficiency in small streams (which determines downstream transport to large streams) and by the spatial pattern of NO_3^- loading to the stream network.

Across biomes, our empirical data show that NO_3^- removal efficiency decreases and downstream export to receiving water bodies increases as NO_3^- concentration increases. Our modelling expands this finding to explain the response of stream networks as land-use intensity increases. Although our replicated inter-biome experiments add substantial insight to NO_3^- dynamics in streams, we do not address some important considerations (see 'Study Limitations' in Supplementary Information) such as the ultimate fate of nitrogen removed from stream water but not immediately denitrified, variation in removal rates with season and stream discharge, the influence of off-channel and subsurface hydrology associated with floodplains and hyporheic flow paths, and the need for *in situ* empirical observations of nitrogen removal in large streams. These uncertainties prevent comparison of results from short-term, *in situ* experiments with annual stream network nitrogen budgets[7,9,19] and therefore represent critical research needs.

Our findings underscore the management imperative of controlling nitrogen loading to streams and protecting or restoring stream ecosystems to maintain or enhance their nitrogen removal functions. Controlling loading to streams and stream nitrogen export is a proven solution to eutrophication and hypoxia problems in downstream inland and coastal waters[23]. Our findings suggest caution before implementing policies (for example, reliance on intensive agriculture for biofuels production[24]) that may yield massive land conversions and higher nitrogen loads to streams. Associated increases in streamwater NO_3^- concentration may reduce the efficacy of streams as nitrogen sinks, yielding synergistic increases in downstream transport to estuaries and coastal oceans[25–27].

METHODS SUMMARY

We added tracer $^{15}NO_3^-$ using standardized protocols to 72 streams across the contiguous United States and Puerto Rico. Within each of eight regions (Supplementary Fig. 1), three streams were bordered by agricultural lands, three by urban areas, and three by extant vegetation typical of the biome ('reference streams') providing a broad array of stream conditions and land-use intensities. We performed these tracer additions on one date in each stream, generally during the spring or summer. We measured NO_3^- uptake rates for entire stream reaches from measurements of tracer ^{15}N in NO_3^-, N_2 and N_2O downstream from the isotope addition based on the nutrient spiralling approach[12,28,29] and a model of denitrification[30].

Our model of NO_3^- removal from water across a stream network accounted for network topology and downstream changes in channel geometry and discharge. We implemented the model using the topology of a fifth-order stream network, the Little Tennessee River in North Carolina, USA. Simulations included increasing NO_3^- loading rates from the catchment to the network from 0.0001 to 100 kg N km^{-2} d^{-1} (yielding input NO_3^- concentrations from 0.15 μg N l^{-1} to 150 mg N l^{-1}). For each NO_3^- loading rate, we conducted model runs using the median observed v_f and allowing v_f to vary with predicted in-stream NO_3^- concentration according to the observed relationship between v_f and NO_3^- concentration (Fig. 2a). These simulations were repeated using the median observed v_{fden} and the v_{fden}–NO_3^- concentration relationship (Fig. 2b). Therefore, model simulations bracket the range of potential network NO_3^- removal (v_f and v_{fden} represent upper and lower limits, respectively). To investigate the importance of stream size on network NO_3^- removal, we categorized streams as either 'small' ($<$100 l s^{-1}, typical of first- and second-order streams) or 'large' (100–6,300 l s^{-1}, typical of third- to fifth-order streams).

Full Methods and any associated references are available in the online version of the paper at www.nature.com/nature.

Received 29 June 2007; accepted 10 January 2008.

1. Vitousek, P. M. *et al.* Human alteration of the global nitrogen cycle: Sources and consequences. *Ecol. Appl.* **7,** 737–750 (1997).
2. Galloway, J. N. *et al.* Nitrogen cycles past, present, and future. *Biogeochemistry* **70,** 153–226 (2004).
3. Aber, J. D. *et al.* Nitrogen saturation in temperate forest ecosystems. *Bioscience* **48,** 921–934 (1998).
4. Bouwman, A. F., Van Drecht, G., Knoop, J. M., Beusen, A. H. W. & Meinardi, C. R. Exploring changes in river nitrogen export to the world's oceans. *Glob. Biogeochem. Cycles* **19,** GB1002, doi:10.1029/2004GB002314 (2005).
5. Johnes, P. J. & Butterfield, D. Landscape, regional and global estimates of nitrogen flux from land to sea: Errors and uncertainties. *Biogeochemistry* **57,** 429–476 (2002).
6. Schlesinger, W. H., Reckhow, K. H. & Bernhardt, E. S. Global change: The nitrogen cycle and rivers. *Water Resource Res.* **42,** W03S06, doi:10.1029/2005WR004300 (2006).
7. Howarth, R. W. *et al.* Riverine inputs of nitrogen to the North Atlantic Ocean: fluxes and human influences. *Biogeochemistry* **35,** 75–139 (1996).
8. Boyer, E. W. *et al.* Riverine nitrogen export from the continents to the coasts. *Glob. Biogeochem. Cycles* **20,** GB1S91, doi:10.1029/2005GB002537 (2006).
9. Van Breemen, N. *et al.* Where did all the nitrogen go? Fate of nitrogen inputs to large watersheds in the northeastern USA. *Biogeochemistry* **57,** 267–293 (2002).
10. Seitzinger, S. P. *et al.* Denitrification across landscapes and waterscapes: a synthesis. *Ecol. Appl.* **16,** 2064–2090 (2006).
11. Hedin, L. O. *et al.* Thermodynamic constraints on nitrogen transformations and other biogeochemical processes at soil–stream interfaces. *Ecology* **79,** 684–703 (1998).
12. Stream Solute Workshop. Concepts and methods for assessing solute dynamics in stream ecosystems. *J. N. Am. Benthol. Soc.* **9,** 95–119 (1990).
13. Dodds, W. K. *et al.* N uptake as a function of concentration in streams. *J. N. Am. Benthol. Soc.* **21,** 206–220 (2002).
14. O'Brien, J. M., Dodds, W. K., Wilson, K. C., Murdock, J. N. & Eichmiller, J. The saturation of N cycling in Central Plains streams: ^{15}N experiments across a broad gradient of nitrate concentrations. *Biogeochemistry*. doi:10.1007/s10533–007–9073–7 (2007).
15. Hall, R. O. & Tank, J. L. Ecosystem metabolism controls nitrogen uptake in streams in Grand Teton National Park, Wyoming. *Limnol. Oceanogr.* **48,** 1120–1128 (2003).
16. Mulholland, P. J. *et al.* Effects of light on NO_3^- uptake in small forested streams: diurnal and day-to-day variations. *J. N. Am. Benthol. Soc.* **25,** 583–595 (2006).
17. Christensen, P. B., Nielsen, L. P., Sørensen, J. & Revsbech, N. P. Denitrification in nitrate-rich streams: Diurnal and seasonal variation related to benthic oxygen metabolism. *Limnol. Oceanogr.* **35,** 640–651 (1990).
18. Piña-Ochoa, E. & Alvarez-Cobelas, M. Denitrification in aquatic environments: A cross-system analysis. *Biogeochemistry* **81,** 111–130 (2006).
19. Alexander, R. B., Smith, R. A. & Schwarz, G. E. Effect of stream channel size on the delivery of nitrogen to the Gulf of Mexico. *Nature* **403,** 758–761 (2000).
20. Peterson, B. J. *et al.* Control of nitrogen export from watersheds by headwater streams. *Science* **292,** 86–90 (2001).
21. Seitzinger, S. P. *et al.* Nitrogen retention in rivers: Model development and application to watersheds in the northeastern USA. *Biogeochemistry* **57,** 199–237 (2002).
22. Wollheim, W. M., Vörösmarty, C. J., Peterson, B. J., Seitzinger, S. P. & Hopkinson, C. S. Relationship between river size and nutrient removal. *Geophys. Res. Lett.* **33,** L06410 (2006).
23. McIsaac, G., David, M. B., Gertner, G. Z. & Goolsby, D. A. Nitrate flux in the Mississippi River. *Nature* **414,** 166–167 (2001).
24. Hill, J., Nelson, E., Tilman, D., Polasky, S. & Tiffany, D. Environmental, economic, and energetic costs and benefits of biodiesel and ethanol biofuels. *Proc. Natl Acad. Sci. USA* **103,** 11206–11210 (2006).
25. Tilman, D., Cassman, K. G., Matson, P. A., Naylor, R. & Polasky, S. Agricultural sustainability and intensive production practices. *Nature* **418,** 671–677 (2002).
26. Foley, J. A. *et al.* Global consequences of land use. *Science* **309,** 570–574 (2005).
27. Beman, J. M., Arrigo, K. R. & Matson, P. A. Agricultural runoff fuels large phytoplankton blooms in vulnerable areas of the ocean. *Nature* **434,** 211–214 (2005).
28. Newbold, J. D., Elwood, J. W., O'Neill, R. V. & Van Winkle, W. Measuring nutrient spiraling in streams. *Can. J. Fish. Aquat. Sci.* **38,** 860–863 (1981).
29. Webster, J. W. & Valett, H. M. in *Methods in Stream Ecology* (eds Hauer, F. R. & Lamberti, G. A.) 169–186 (Elsevier, New York, 2006).
30. Mulholland, P. J. *et al.* Stream denitrification and total nitrate uptake rates measured using a field ^{15}N isotope tracer approach. *Limnol. Oceanogr.* **49,** 809–820 (2004).

Supplementary Information is linked to the online version of the paper at www.nature.com/nature.

Acknowledgements Funding for this research was provided by the National Science Foundation. We thank N. Ostrom for assistance with stable isotope measurements of N_2 and N_2O, and W. Wollheim for initial development of the model that we modified to estimate denitrification rates from field data. We thank M. Mitchell, B. Roberts and E. Bernhardt for their comments on earlier versions of the paper. We thank the NSF LTER network, US Forest Service, National Park Service and many private landowners for permission to conduct experiments on their lands. Partial support to P.J.M. during manuscript preparation was provided by the US Department of Energy, Office of Science, Biological and Environmental Research under contract with UT-Battelle.

Author Contributions P.J.M. coordinated the stream ^{15}N experiments and analysed the compiled experimental data sets. A.M.H. and G.C.P conducted the stream network modelling. P.J.M., A.M.H. and G.C.P. wrote major portions of the manuscript. S.K.H. established sampling protocols and coordinated the ^{15}N analysis of dissolved N_2 samples. Except for A.M.H., all authors listed to J.R.W. were joint project Principal Investigators and contributed to the conceptual and methodological development of the project and analysis of data. Authors listed from C.P.A. to S.M.T. coordinated field experiments and analysed data from one or more biomes. All authors discussed the results and commented on the manuscript.

Author Information Reprints and permissions information is available at www.nature.com/reprints. Correspondence and requests for materials should be addressed to P.J.M. (mulhollandpj@ornl.gov).

METHODS

The second Lotic Intersite Nitrogen Experiment (LINX II) consisted of a series of ^{15}N tracer additions to streams across multiple biomes and land use conditions in the United States and Puerto Rico to provide *in situ*, reach-scale measurements of total nitrate (NO_3^-) uptake and denitrification. Identical protocols were followed at all sites for experimental design and measurement of NO_3^- uptake and denitrification rates, hydraulic and other physical parameters, nutrients, reach-scale rates of metabolism, biomass in various compartments, and stable isotope ratios. We generally followed the methods outlined in a prior ^{15}N-NO_3^- addition study in Walker Branch, Tennessee[30]. Detailed sampling, sample processing and analysis, and calculation protocols for the LINX II study are available at the project website (http://www.biol.vt.edu/faculty/webster/linx/). Selection of study streams, including location and environmental conditions, is presented in Supplementary Fig. 1 and Supplementary Table 1.

Isotope additions. We continuously added a $K^{15}NO_3$ ($\geq$98% ^{15}N) solution to each stream over a 24-h period using a peristaltic or fluid metering pump. The isotope addition was designed to achieve a 20-fold increase in the ^{15}N:^{14}N ratio of streamwater NO_3^-. This level of isotope addition resulted in a small ($\sim$7.5%) increase in the concentration of NO_3^- in stream water. We added NaCl or NaBr to the isotope solution as a conservative tracer to account for downstream dilution due to groundwater input and to measure water velocity and channel hydraulic properties. The isotope additions were started at $\sim$13:00 local time in each stream. Within 1 day of the isotope additions we conducted propane or SF_6 injections to measure air–water gas exchange rates.

Stream sampling and isotope analysis. Stream reaches of 105 to 1,830 m (reach length was dependent on stream size) were sampled at six to ten locations downstream from the isotope addition. We measured tracer ^{15}N flux in NO_3^-, N_2 and N_2O downstream from the addition point after downstream concentrations reached steady state. Samples for ^{15}N were collected once several hours before (to determine natural abundance ^{15}N levels) and twice after the isotope addition commenced: at $\sim$12 h (near midnight) and $\sim$23 h (near noon). We determined ^{15}N-NO_3^- on filtered samples using a sequential reduction and diffusion method[31]. Samples were analysed for ^{15}N on either a Finnigan Delta-S or a Europa 20/20 mass spectrometer in the Mass Spectrometer Laboratory of the Marine Biological Laboratory in Woods Hole, MA (http://ecosystems.mbl.edu/SILAB/aboutlab.html), a Europa Integra mass spectrometer in the Stable Isotope Laboratory of the University of California, Davis (http://stableisotopefacility.ucdavis.edu/) or a ThermoFinnigan DeltaPlus mass spectrometer in the Stable Isotope Laboratory at Kansas State University (http://www.k-state.edu/simsl).

Water samples for ^{15}N-N_2 and ^{15}N-N_2O were collected at each sampling location, equilibrated with helium in 60- or 140-ml syringes, and injected into evacuated vials using underwater transfers of sample and gas to reduce the potential for any air contamination[32]. Gas samples were analysed for ^{15}N by mass spectrometry either using a Europa Hydra Model 20/20 mass spectrometer at the Stable Isotope Laboratory of the University of California, Davis, or a GV Instruments Prism Series II mass spectrometer in the Biogeochemistry Laboratory, Department of Zoology, Michigan State University. The ^{15}N content of all samples was reported in $\delta^{15}N$ notation where $\delta^{15}N = [(R_{SA}/R_{ST}) - 1] \times 1{,}000$, $R = {}^{15}N/{}^{14}N$, and the results are expressed as per mil (‰) deviation of the sample from the standard N_2 in the atmosphere ($\delta^{15}N = 0$‰). All $\delta^{15}N$ values were converted to mole fractions (MF) of ^{15}N ($^{15}N/(^{14}N+{}^{15}N)$), and tracer ^{15}N fluxes were calculated for each sample by multiplying the ^{15}N mole fractions, corrected for natural abundances of ^{15}N by subtracting the average ^{15}N mole fractions for samples collected before the ^{15}N addition, by the concentrations of NO_3^-, N_2, or N_2O in stream water (concentrations of NO_3^- and N_2O were measured, whereas N_2 was taken as the concentration in equilibrium with air at the ambient stream temperature), and stream discharge derived from the measured conservative solute tracer concentrations.

NO_3^- uptake and denitrification rates. We measured NO_3^- uptake rates for entire stream reaches based on the nutrient spiralling approach[28,29] and calculated several metrics describing NO_3^- uptake, including uptake length, uptake velocity and areal uptake rate[12]. Details are provided in the Supplementary Information.

Statistical analysis. To improve normality before parametric statistical analysis all NO_3^- uptake parameters and other variables were log-transformed, with the exception that denitrification fraction was arcsine-square root transformed. Effect of land-use category was determined using analysis of variance (ANOVA) and non-parametric tests on untransformed data. All statistical tests were performed using SAS®, Version 9.1 for Windows (SAS Institute, Inc.).

Stream network model. We developed a simulation model of NO_3^- loading, transport, and biotic uptake within stream networks, and used the model to investigate how NO_3^- removal in stream networks responds to increased loading. The model routes NO_3^- and water from the landscape and through a stream network, and biological uptake removes NO_3^- from the stream water in each reach. Details of model structure and parameterization are presented in the Supplementary Information.

Model runs. The model was implemented for 28 different NO_3^- loading rates to streams under four different v_f scenarios, for a total of 112 model runs. Water yield per unit catchment area was constant for the stream network across all NO_3^- loading rates and v_f scenarios. Nitrate loading rate to streams (and, because the water yield was constant, the incoming NO_3^- concentration) was constant across the stream network for each model simulation. Model simulations included systematically increasing NO_3^- loading rates from the catchment to the stream network from 0.0001 to 100 kg N km^{-2} d^{-1} (yielding input NO_3^- concentrations ranging from 0.15 μg N l^{-1} to 150 mg N l^{-1}). For each NO_3^- loading rate, we conducted model runs using a constant v_f (median observed value) and allowing v_f to vary with predicted in-stream NO_3^- concentration according to the observed relationship between v_f and NO_3^- concentration. These simulations were repeated for v_{fden} (see main text and Supplementary Table 3).

To investigate the relative importance of stream size on NO_3^- removal, we categorized stream reaches as either 'small' ($<$100 l s^{-1}, typical of first- and second-order streams) or 'large' (100–6,300 l s^{-1}, typical of third- to fifth-order streams). Small streams account for 77% of stream length and 50% of streambed surface area across the stream network (see Supplementary Fig. 3). Because we arbitrarily defined distribution of streambed area among 'small' and 'large' categories, the magnitude of NO_3^- removal in small versus large streams (Fig. 4c) is also arbitrary and we focused our analysis on the relative change in the ratio as NO_3^- loading increases.

31. Sigman, D. M. *et al.* Natural abundance-level measurement of the nitrogen isotopic composition of oceanic nitrate: an adaptation of the ammonia diffusion method. *Mar. Chem.* **57**, 227–242 (1997).
32. Hamilton, S. K. & Ostrom, N. E. Measurement of the stable isotope ratio of dissolved N_2 in ^{15}N tracer experiments. *Limnol. Oceanogr. Methods* **5**, 233–240 (2007).

SUPPLEMENTARY INFORMATION

SUPPLEMENTARY METHODS

Selection of study streams. We selected streams in order to include a wide range of biomes and land use types. In each of 8 regions representing different biomes (Supplementary Figure 1) we chose three headwater streams (1st and 2nd order) in each of three land-use categories (reference, agricultural, urban), for a total of 72 streams (Supplementary Table 1). Streams were assigned to land-use categories based on visual observation of the dominant land use adjacent to the study reach. Reference streams were bordered by native vegetation according to biome and included forests, grassland, and desert/shrub vegetation. Agricultural streams included a wide variety of cultivated lands, open range grazing, and pastures. Urban streams included those bordered by housing developments, golf courses, urban commercial areas with a few cement-lined channels. Determination of land cover in the catchments of each stream (using the USGS National Elevation Data Set, available at http://seamless.usgs.gov, and 2001 USGS National Land Cover Datasets, available online at http://seamless.usgs.gov, or for the PR streams from 1991-1992 Landsat TM imagery as derived by Helmer et al.[33] showed that reference streams drained catchments with >85% native vegetation (except for 2 streams with 50 and 65% native vegetation), whereas agricultural and urban streams drained catchments ranging from <1 to 100% agricultural and urban land cover types.

Measurement of NO_3^- uptake and denitrification rates. We measured NO_3^- uptake rates for entire stream reaches based on the nutrient spiraling approach[16, 28, 29]. Total NO_3^- uptake was determined from the downstream rate of decline in tracer $^{15}NO_3^-$ mass flux using the model:

$$d^{15}NO_3^-/dx = -k_{tot} * {}^{15}NO_3^- \quad (1)$$

where $^{15}NO_3^-$ is the tracer $^{15}NO_3^-$ flux (μg ^{15}N s^{-1}), x is the stream channel distance from the tracer addition (m), and k_{tot} is the distance-specific NO_3^- uptake rate (m^{-1}). We were able to determine k_{tot} for 69 of the 72 streams studied.

Denitrification rates (calculated separately for production of N_2 and N_2O) were estimated by fitting a model of N gas production to the measured fluxes of tracer ^{15}N as N_2 and N_2O over the study reach as follows:

$$d^{15}NO_3^-/dx = -(k_{den}+k_U)^{15}NO_3^- \quad (2)$$

$$d^{15}N_{GAS}/dx = k_{den}{}^{15}NO_3^- - k_2{}^{15}N_{GAS} \quad (3)$$

where $^{15}NO_3^-$ is the tracer ^{15}N flux in NO_3^- (μg ^{15}N s^{-1}) and $^{15}N_{GAS}$ is the tracer ^{15}N flux in N_2 or N_2O (ng ^{15}N s^{-1}), k_{den} is the distance-specific N_2 or N_2O production rate (m^{-1}), k_U is the assimilative uptake rate of NO_3^- (m^{-1}), and k_2 is the air-water exchange of N_2 or N_2O. Values of k_2 for N_2 and N_2O were calculated from the measured rates of evasion of propane or SF_6 and the relative values of their Schmidt numbers[34]. Because the total

uptake rate of NO_3^- (k_{tot}) is the sum of denitrification and assimilatory uptake (i.e., $k_{den}+k_U$), the equations above were solved only for k_{den} using the optimization tool "Solver" in Microsoft Office Excel.

Denitrification rates (k_{den}) were measured by model fitting only when there was significant tracer ^{15}N in N_2 or N_2O (defined as $\delta^{15}N$ values greater than the upper 97.5% confidence interval of background values measured prior to the isotope addition) at 3 or more stations along the stream reach. We then calculated a confidence range in the parameters using Maximum Likelihood Estimate (MLE)[35] to each of the model fits to ensure k_{den} values were significantly greater than 0 (i.e., 95% confidence interval of k_{den} did not include 0). We also applied MLE to ^{15}N flux data from streams that did not meet the model fitting criterion above (3 stations with significant tracer ^{15}N in N_2 or N_2O) to determine if k_{den} was sufficiently constrained to assign a non-zero value. This procedure resulted in the determination of k_{den} for 49 and 53 streams for N_2 and N_2O production, respectively. N_2 production rates far exceeded N_2O production rates in all streams, with median N_2 production rate being 99.4% of the sum of N_2 and N_2O production rate (range of 94.3 to 99.9%). Total k_{den} was then calculated as the sum of the k_{den} values for N_2 and N_2O for the 49 streams with measurable N_2 production rates.

Total uptake and denitrification rates reported for each stream are the average of the rates measured for the two sampling periods. On average, k_{tot} was 55% higher for the second sampling (near noon) than the first sampling (near midnight), and this difference was significant ($P < 0.01$, t-test, SAS Proc Means, SAS®, Version 9.1 for Windows, SAS Institute, Inc., Cary, NC, USA). Differences in k_{den} for both N_2 and N_2O production between sampling periods were not statistically different, however.

Physical, chemical, and biological variables were measured in each stream during or within 1 day of the ^{15}N experiment to determine potential predictors of total NO_3^- uptake and denitrification rates. Detailed sampling and analysis methods are available at the LINX project website (http://www.biol.vt.edu/faculty/webster/linx/). Average stream width (w) was determined from measurements of wetted width at 5-10 m intervals along the experimental reach. Average discharge was measured by dilution of the conservative solute tracer. Average water velocity was measured by the time of travel of the rising limb of the conservative tracer profile and average depth was determined by discharge/(width × velocity). An advection-dispersion model with transient storage was applied to the conservative tracer data to determine hydraulic characteristics related to transient storage zones[36]. We measured concentrations of NO_3^- (either by ion chromatography or by azo dye colorimetry after Cu-Cd reduction), NH_4^+(by phenate colorimetry or fluorometry), total soluble N (TSN, high temperature combustion, Shimadzu TOC-V with total Nitrogen Module), soluble reactive phosphorus (SRP, ascorbic acid-molybdenum blue), and dissolved organic carbon (DOC, high temperature combustion, Shimadzu TOC-V). Concentrations of dissolved organic N (DON) were estimated as the difference between TSN and the sum of NH_4^+ and NO_3^-. Abundance of several benthic organic matter components (coarse and fine benthic organic matter, epilithon, bryophytes, filamentous algae, vascular plants) was determined by collecting materials from known areas of the stream bottom at 5-10 locations within the study reach and measurement of dry mass (60°C) and ash-free dry mass (after combustion at 500°C) of the material collected. Reach-scale rates of metabolism (gross primary production,

GPP, and ecosystem respiration, ER) were measured using the diel dissolved oxygen method[37].

Calculation of nutrient spiraling metrics. We calculated several additional spiraling metrics for NO_3^- uptake from k_{tot} and k_{den} (ref [16]). Nitrate uptake length (S_W) was calculated from the rate of decline of tracer [^{15}N] NO_3^- flux (μg ^{15}N s^{-1}) over distance downstream from the addition site. Tracer [^{15}N] NO_3^- flux at each sampling station was determined from the $\delta^{15}N$, NO_3^- concentration, and discharge at each station, corrected for background values based on measurements just prior to the experiment. S_W was determined from the negative inverse of the slope (k_{tot}) of natural log-transformed tracer [^{15}N] NO_3^- fluxes versus distance [$S_W = -1/k_{tot}$, where k_{tot} is the distance-specific uptake rate (m^{-1})]. Values of k_{tot} were determined for the total removal of NO_3^- from water as well as for the NO_3^- removal by denitrification (k_{den}) as indicated by $^{15}N_2$ and $^{15}N_2O$ gas fluxes. To compare biotic nutrient removal among streams, we calculated uptake velocity because, unlike uptake rates per unit distance (k_{tot}, k_{den}), uptake velocity is independent of the effects of water transport rate[16]. Uptake velocity (υ_f) was calculated as: $\upsilon_f = (v \times h)/S_W$, = Q/(10 × w × S_W), where v = water velocity (cm s^{-1}), h = water depth (m), S_W = uptake length (m), Q = discharge (L s^{-1}), and w = average stream wetted width (m). Areal uptake rate (U, μg m^{-2} h^{-1}) was calculated as: $U = (\upsilon_f \times C) \times 36000$, where C is the ambient NO_3^- concentration (μg N L^{-1}) and 36000 is a conversion factor. Uptake length, uptake velocity, and aerial uptake rate for denitrification (S_{Wden}, υ_{fden}, and U_{den}, respectively) were determined in the same way, except that k_{den} was used rather than k in the calculations.

Stream network model structure. We developed a simulation model of NO_3^- loading, transport, and biotic uptake within streams. The model routes NO_3^- and water from the landscape and through a stream network from the headwaters to the outlet, and biological uptake removes NO_3^- from the water column in each stream reach (Supplementary Figure 2).

The model calculates the mass of NO_3^- and discharge (Q) with a simple steady-state mass-balance approach in which incoming fluxes are subtracted from outgoing fluxes for each stream reach. Discharge for each reach is calculated by subtracting outgoing water fluxes from incoming water fluxes according to the following equation (terms defined in Supplementary Table 2):

$$Q_p = \overset{\text{inflows}}{(\Sigma Q_{p\text{-}1_i} + Q_L)} - \overset{\text{outflows}}{(Q_w + Q_{p+1_i})} \quad (4)$$

$$\text{where } Q_L = A_p \cdot Y_p \quad (5)$$

Nitrate for each reach is calculated similarly by subtracting outgoing nitrate from incoming nitrate fluxes as follows (terms defined in Supplementary Table 2):

$$NO_3^-{}_p = \overset{\text{inflows}}{(\Sigma\, NO_3^-{}_{p\text{-}1_i} + NO_3^-{}_L)} - \overset{\text{outflows}}{(NO_3^-{}_R + NO_3^-{}_{p+1_i})} \quad (6)$$

$$\text{where } NO_3^-{}_L = A_p \cdot L_p \quad (7)$$

For each stream reach, the mass of nitrate removed ($NO_3^-_R$) is equal to the nitrate in the stream reach times the fractional removal of nitrate:

$$NO_3^-_R = R * NO_3^-_p \quad (8)$$

The fractional removal (R) is determined by the following equation recently applied by Wollheim et al.[15] (terms defined in Supplementary Table 2):

$$R = 1 - e^{(-vf/H_L)} \quad (9)$$

$$\text{where } H_L = Q_p / SA_p \quad (10)$$

The surface area (SA, L^2) equals the stream reach length (l) multiplied by average width (w), where the average width of a stream segment is estimated based on the equation of Leopold and Maddock[38] (terms defined in Supplementary Table 2):

$$w = aQ^b \quad (11)$$

Model parameterization. The stream network topology was parameterized using the 5th-order Little Tennessee River network in western North Carolina and northeastern Georgia (Supplementary Figure 3). Digital stream networks were derived by using 30-meter raster digital elevation models (USGS National Elevation Data Set, http://seamless.usgs.gov) and the Hydrologic Modeling extension in ArcView GIS software (Version 3.3, ESRI, Redlands, CA 2002). The stream network derived from the DEM was similar to the 1:24,000- scale stream network derived from USGS quadrangles. The stream network was divided into segments, defined as the length of stream between tributary junctions. Segments were divided into approximately 500-meter reaches, which yielded 1722 stream reaches. Model parameters were derived as described in Supplementary Table 3.

SUPPLEMENTARY DISCUSSION

Nitrate removal over a standardized stream reach. Across our streams, total uptake resulted in 72% removal of nitrate inputs from water over a standardized 1 km stream reach (median value, lower and upper quartile values of 34% and 98%, respectively). Denitrification resulted in 10% nitrate removal (median, lower and upper quartile values of 4% and 22%, respectively). Nitrate removal presented in this way (as a fractional removal rate per unit distance as determined directly from our measurements, k_{tot} and k_{den}, Supplementary table 1) is a function of both hydrology (rate of water transport) and biology (rate of uptake, primarily by benthic organisms). There was no significant effect of land use on the fractional removal rate per unit distance (Kruskal-Wallis test, SAS®, Version 9.1 for Windows, SAS Institute, Inc., Cary, NC, USA) because transport rate (discharge) varied by several orders of magnitude among streams within each land use category resulting in high variability in fractional removal rate within each category. We

did observe significant inverse correlations (Pearson Correlations, SAS®, Version 9.1 for Windows, SAS Institute, Inc., Cary, NC, USA) between k_{tot} and water discharge per unit stream width (Q/w) (r = - 0.453, P < 0.0001, log-transformed values) and between k_{den} and Q/w (r = - 0.308, P = 0.031, log-transformed values) as expected based on spiraling theory[16]. Stream discharge was unrelated to land use category (Kruskal-Wallis test, SAS®, Version 9.1 for Windows, SAS Institute, Inc., Cary, NC, USA); thus, variations in discharge did not bias our analysis of land use category effects.

Study limitations. Although our inter-biome experiments and stream network modeling results add considerable insight to in-stream NO_3^- dynamics, many limitations arise from both field methodologies and model assumptions that affect our ability to extrapolate our results both temporally and spatially. Our experimental approach did not quantify the ultimate fate of $^{15}NO_3^-$ assimilated but not immediately denitrified. This $^{15}NO_3^-$ will not be stored indefinitely on the streambed, but eventually will be denitrified, re-released as some form of dissolved N to the water column, or transported downstream as particulate N. Furthermore, all tracer additions were conducted at or near steady-state hydrologic conditions, and typically at or near annual low flows. High rates of nutrient transport typically occur during infrequent high flows whereas high rates of biological assimilation and storage typically occur during frequent low flows in streams[39], and rates of biological assimilation may be higher in the summer when temperatures are warmer and there is greater biological activity. Therefore, our experimental design, although based on state-of-the-art methods for measuring N processing in streams, prevents extrapolation of our results to annual N processing rates.

We are also limited in our ability to scale empirical results spatially across diverse steam networks. The structure of our stream network model does not include spatial variation in N inputs from the landscape, yet the spatial distribution of N sources in a watershed may drive patterns of N removal[12,14]. The representation of hydrogeomorphology in our stream network model also prevents us from extrapolating our model results to systems in which the channel is extensively hydrologically connected to off-channel (floodplain or wetlands) or subsurface (hyporheic zone or groundwater) systems, which may be important determinants of N removal within streams[40,41,42]. Finally, because our empirical results are based on experiments conducted only in small streams (0.2 – 267 Ls^{-1}; Supplementary Table 1) there is some uncertainty in extrapolating these results to larger systems, even though our model accounts for expected changes channel cross section (which influences the relationship between discharge and stream bed area). The general lack of *in situ* measurements of uptake and denitrification rates in large streams further adds to this uncertainty.

SUPPLEMENTARY NOTES

33. Helmer, E. H., Ramos, O., Lopez, T.D.M., Quinones, M, & Diaz, W. Mapping the forest type and land cover or Puerto Rico, a component of the Caribbean Biodiversity Hotspot. *Caribbean Journal of Science* **38**, 165-183 (2002)

34. MacIntyre, S., Wanninkhof, R. & Chanton, J. P. in *Biogenic trace gases: Measuring Emissions from Soil and Water* (eds Matson, P.A. & Harriss, R. C.) 52-97 (Blackwell, 1995).

35. Hilborn, R. & Mangel, M. *The ecological detective: confronting models with data* (Princeton University Press, Princeton, 1997).

36. Bencala, K. E. & Walters, R. A. Simulation of solute transport in a mountain pool-and-riffle stream: a transient storage model. *Water Resourc. Res*., **19**, 718-724 (1983).

37. Bott, T. L. in *Methods in Stream Ecology* (eds Hauer, F. R. & Lamberti, G. A.) 663-690 (Elsevier, New York, 2006).

38. Leopold, L.B & Maddock, T. The hydraulic geometry of streams and some physiographic implications. U.S.G.S. Professional Paper 252 (1953).

39. Royer, T. V., Tank, J. L. & David, M. B. Transport and Fate of Nitrate in Headwater Agricultural Streams in Illinois. *Journal of Environmental Quality* **33**,1296-1304 (2004)

40. Valett, H. M., Morrice, J. A., Dahm, C. N., & Campana, M.E. Parent Lithology, Surface-Groundwater Exchange, and Nitrate Retention in Headwater Streams. *Limnology and Oceanography* **41**, 333-345 (1996)

41. Findlay, S. Importance of Surface-Subsurface Exchange in Stream Ecosystems: The Hyporheic Zone. *Limnology and Oceanography* **40**,159-164 (1995)

42. Naiman, R.J. & Decamps, H. The ecology of interfaces: riparian zones. *Annual Review of Ecology and Systematics* **28**, 621-658 (1997)

Supplementary Table 1: Locations and mean physical and chemical characteristics of LINX II streams on the day of the ^{15}N experiments.

Region (biome)	Stream name	Land use	Latitude	Longitude	^{15}N expt date	Discharge ($L\ s^{-1}$)	Width (m)	Velocity ($m\ min^{-1}$)	Depth (m)	Water temp (^{o}C)	NO_3^- ($ug\ N\ L^{-1}$)	NH_4^+ ($ug\ N\ L^{-1}$)	SRP ($ug\ L^{-1}$)	DOC ($mg\ L^{-1}$)	k_{tot} (m^{-1})	k_{den} (m^{-1})
MA	Cart §	REF	42.77133	-70.91995	7/15/2003	4.8	2.5	0.6	0.18	17.9	15	293	1	8.7	0.0028	
(Northern	IS_104	URB	42.53797	-71.20925	7/29/2003	2.1	1.3	0.9	0.11	17.1	1336	121	2	2.8	0.0007	0.0004
deciduous	Boxford	REF	42.64177	-70.99430	7/27/2004	12.2	1.5	4.0	0.12	19.8	53	13	9	6.8	0.0007	0.0002
forest)	Runaway	AGR	42.64763	-70.85970	6/29/2004	0.7	0.6	1.1	0.07	16.3	1164	80	8	2.1	0.001	0.0003
	Long Meadow	AGR	42.65252	-70.84800	7/13/2004	2.4	1.1	2.2	0.06	16.6	989	63	11	3.5	0.0006	0.0005
	Gravelly * §	REF	42.66302	-70.90089	8/9/2005	2.0	2.5	1.1	0.04	21.4	112	435	80	25.6		
	Black	AGR	42.64428	-70.87115	7/12/2005	120.1	2.6	2.5	1.12	22.6	50	31	34	13.9	0.0003	7E-05
	Sawmill	URB	42.52238	-71.18600	7/26/2005	4.9	2.7	0.8	0.15	21.2	1025	39	11	10.0	0.0002	0.0002
	IS_118	URB	42.58234	-71.07825	7/7/2005	11.3	1.7	4.1	0.09	18.7	513	254	12	12.5	0.0002	0.0002
NC	Hugh White §	REF	35.04955	-83.43058	5/23/2003	19.4	3.7	6.7	0.05	12.7	7	3	3	0.4	0.0024	
(Southern	Hoglot * §	AGR	35.09324	-83.38626	6/10/2003	52.7	1.7	11.8	0.16	17.6	154	17	3	0.6		
deciduous	Crawford §	URB	35.17988	-83.40549	6/20/2003	45.0	1.5	8.3	0.21	17.3	103	15	4	0.6	0.0001	
forest)	Big Hurricane	REF	35.06897	-83.44340	5/20/2004	12.2	2.4	2.6	0.12	14.7	241	6	3	0.5	8E-05	3E-05
	Jerry	AGR	34.95625	-83.40396	6/22/2004	26.5	1.8	9.1	0.09	18.0	406	108	18	1.6	5E-05	3E-05
	Mud	URB	34.98761	-83.31690	6/16/2004	51.8	1.9	13.6	0.12	16.7	140	6	2	1.4	0.0002	5E-06
	Cunningham	REF	35.04964	-83.45510	6/3/2005	49.3	2.3	7.1	0.19	12.7	10	3	2	0.9	0.001	0.0007
	Blacks	AGR	34.94276	-83.38099	6/16/2005	189.4	1.9	29.5	0.20	16.1	173	8	7	0.8	0.0001	1E-05
	Sugarloaf	URB	35.37986	-83.11826	6/9/2005	79.8	2.3	13.8	0.15	13.8	54	3	3	0.9	0.0002	0.0001
MI	Sand	REF	42.57838	-85.92831	6/18/2003	4.9	1.1	6.7	0.04	15.1	283	55	15	4.3	0.001	0.0002
(Northern	Steinke	AGR	42.70768	-85.69205	6/5/2003	1.7	1.2	4.3	0.02	12.3	4158	29	68	18.7	0.0025	1E-05
deciduous	Dorr	URB	42.72748	-85.72134	6/12/2003	35.0	1.4	8.6	0.17	12.4	1100	128	9	2.4	0.0002	3E-05
forest)	Bullet	REF	42.29769	-85.36161	5/5/2004	6.5	1.4	5.9	0.05	12.6	384	11	2	1.2	0.0005	0.0004
	Buskirk	AGR	42.63578	-85.66225	8/5/2004	6.0	0.9	10.5	0.04	17.9	82	21	11	8.2	0.0023	9E-05
	Wayland	URB	42.67094	-85.66053	6/16/2004	11.7	1.2	7.0	0.09	17.8	695	74	5	7.4	0.0004	8E-05
	Honeysuckle* §	REF	42.30852	-85.34023	6/1/2005	99.4	3.2	11.6	0.16	22.2	4	21	4	4.2		
	Bellingham	AGR	42.49301	-85.57034	5/11/2005	22.9	1.2	15.9	0.07	11.8	1453	28	2	3.0	0.0001	6E-06
	Arcadia	URB	42.27308	-85.61664	6/20/2005	110.1	2.5	10.1	0.26	20.0	274	32	11	2.8	0.0007	4E-05
KS	Kings N4D	REF	39.08792	-96.58443	5/21/2003	13.4	2.4	5.0	0.07	13.5	9	0	1	0.7	0.0062	0.0003
(Tallgrass	Agnorth §	AGR	39.21247	-96.59275	6/11/2003	0.2	0.8	1.1	0.02	21.5	35	32	0	4.2	0.0061	
prairie)	Campus	URB	39.19273	-96.57873	7/1/2003	2.9	2.6	0.9	0.08	25.5	2942	8	4	4.2	0.0014	3E-05
	K2A §	REF	39.10017	-96.57388	6/30/2004	26.3	2.5	6.7	0.09	17.4	1	7	2	0.8	0.0077	
	Natalie §	AGR	39.22860	-96.65893	6/22/2004	1.3	1.2	1.6	0.04	20.4	6	3	2	1.6	0.0147	
	Walmart Ditch	URB	39.18540	-96.55830	5/27/2004	1.6	2.1	0.9	0.05	27.1	277	28	35	3.8	0.0079	0.0028
	Shane §	REF	39.11293	-96.55552	5/17/2005	4.4	2.4	1.2	0.09	14.9	1	5	1	0.5	0.0507	
	Swine	AGR	39.21823	-96.57409	6/27/2005	5.4	1.6	2.8	0.07	20.8	21162	3	16	2.4	0.0019	4E-05
	Little Kitten	URB	39.20579	-96.63429	6/8/2005	20.1	3.3	2.7	0.14	19.7	168	24	7	1.7	0.0013	0.0002

Supplementary Table 1 (continued): Locations and mean physical and chemical characteristics of LINX II streams on the day of the ^{15}N experiments.

Region (biome)	Stream name	Land use	Latitude	Longitude	^{15}N expt date	Discharge ($L\ s^{-1}$)	Width (m)	Velocity ($m\ min^{-1}$)	Depth (m)	Water temp (^oC)	NO_3^- ($ug\ N\ L^{-1}$)	NH_4^+ ($ug\ N\ L^{-1}$)	SRP ($ug\ L^{-1}$)	DOC ($mg\ L^{-1}$)	k_{tot} (m^{-1})	k_{den} (m^{-1})
WY	Ditch §	REF	43.66346	-110.62764	7/8/2003	55.7	4.7	11.7	0.06	16.8	0	2	2	2.2	0.0039	
(Dry	Giltner §	AGR	43.54900	-110.84028	7/4/2003	158.5	5.7	10.2	0.16	12.0	50	3	3	2.0	0.0057	
coniferous	Golf §	URB	43.56670	-110.75230	7/20/2003	110.0	2.6	14.4	0.18	18.6	1	1	2	0.3	0.0039	
forest)	Two Oceans	REF	43.87618	-110.48765	7/17/2004	64.5	2.9	15.6	0.09	12.8	19	4	10	1.3	0.0022	0.0002
	Headquarters	AGR	43.56765	-110.80033	7/10/2004	131.1	5.2	9.6	0.16	16.0	1	3	15	0.8	0.0118	0.0058
	Teton Pines	URB	43.53045	-110.84283	7/14/2004	9.5	2.4	2.8	0.08	10.9	152	1	3	0.4	0.0018	4E-05
	Spread §	REF	43.78808	-110.53155	7/19/2005	267.8	6.6	16.0	0.15	14.3	3	2		1.6	0.0024	
	Kimball	AGR	43.56722	-110.81687	7/6/2005	153.8	4.6	9.3	0.22	11.2	28	1	4	0.7	0.0035	0.0001
	FISH	URB	43.58463	-110.82771	7/12/2005	102.9	2.2	8.8	0.31	9.9	235	4	6	0.3	0.0004	3E-05
SW	Agua Fria	REF	34.35160	-112.10410	5/15/2003	11.9	3.1	8.0	0.03	18.0	0	2	56	0.9	0.0251	0.0101
(Desert)	Bernalillo §	AGR	35.32670	-106.54710	6/20/2003	23.5	2.9	2.8	0.17	18.6	2	2	37	1.8	0.0132	
	Rancho §	URB	35.19790	-106.64450	7/16/2003	17.8	4.4	2.0	0.12	23.3	13	3	50	2.4	0.0107	
	Salado §	REF	34.33580	-107.03920	5/22/2004	5.8	3.7	6.4	0.01	18.0	4	4	3	1.0	0.0044	
	Puerco	AGR	34.40980	-106.85380	5/9/2004	2.5	1.3	1.4	0.08	20.5	4	4	14	3.8	0.0204	0.0002
	San Pedro	AGR	35.20770	-106.30900	7/2/2004	4.0	2.0	7.4	0.02	16.3	297	4	19	0.9	0.0035	0.0008
	Sycamore	REF	33.75330	-111.50600	7/6/2005	21.3	3.7	13.5	0.03	25.4	58	2	32	2.2	0.0054	0.0001
	Indian Bend Wash §	URB	33.47281	-111.91532	11/2/2003	28.4	4.8	1.6	0.23	20.0	99	65	21		0.0002	
	Tempe Town lake	URB	33.43370	-111.94900	4/17/2004	18.0	4.1	1.0	0.25	22.2	4	10	25	1.0	0.0069	0.0001
OR	Oak §	REF	44.61143	-123.33049	8/26/2003	7.5	2.1	2.8	0.08	15.1	71	1	35	2.0	0.0011	
(Wet	Oak	AGR	44.56827	-123.30289	8/13/2003	5.5	2.7	0.7	0.19	17.3	96	8	48	10.1	0.0015	7E-05
coniferous	Oak	URB	44.55859	-123.28514	7/30/2003	5.6	3.9	0.4	0.23	20.3	163	19	45	1.9	0.0011	0.0002
forest)	Mack §	REF	44.21657	-122.16369	8/31/2004	30.7	6.7	5.6	0.05	12.5	63	6	13	0.9	0.0006	
	Camp	AGR	44.11541	-122.81954	7/28/2004	113.4	5.9	4.6	0.25	17.6	54	6	5	0.9	0.0002	6E-05
	Amazon §	URB	44.04388	-123.09453	7/7/2004	25.0	6.4	3.4	0.07	21.1	2	5	18	3.4	0.01	
	Potts §	REF	44.26377	-122.48923	7/28/2005	19.0	2.9	5.0	0.08	13.7	69	4	25	1.3	0.0005	
	Courtney	AGR	44.36367	-122.96750	7/13/2005	34.7	3.3	3.3	0.19	18.9	97	11	5	2.6	0.0018	0.0002
	Periwinkle §	URB	44.61951	-123.07788	8/17/2005	2.7	3.4	0.3	0.19	22.6	8	4	209	7.0	0.0407	
PR	Bisley	REF	18.31650	-65.74835	2/4/2004	12.5	3.2	2.4	0.10	21.3	171	3	22	0.6	0.001	0.0005
(Tropical	Grande	AGR	18.15932	-65.95035	2/19/2004	12.3	1.0	10.9	0.07	23.0	276	11	13	1.8	0.0007	3E-05
forest)	Petunia	URB	18.38523	-66.08513	2/27/2004	4.7	1.8	1.4	0.11	24.3	997	15	26	1.5	0.0008	0.0003
	RIT	REF	18.28048	-65.78925	2/24/2005	20.0	1.2	5.8	0.17	19.0	131	7	0	0.3	0.0002	2E-05
	Maizales	AGR	18.23354	-65.75931	2/11/2005	25.0	3.5	1.6	0.26	23.0	206	7	12	0.9	0.0022	4E-05
	Mtrib	URB	18.37040	-65.77972	2/2/2005	23.2	2.5	1.4	0.41	20.8	174	2204	311	2.2	0.001	0.001
	Pared	REF	18.33409	-65.82162	2/23/2006	5.2	2.7	1.1	0.10	22.1	105	3	7	1.3	0.0032	4E-05
	Vaca	AGR	18.34340	-65.84181	2/11/2006	111.9	2.0	3.6	0.94	23.0	446	3	9	1.0	0.0001	9E-05
	Ceiba	URB	18.27135	-65.64887	2/6/2006	49.5	2.7	4.1	0.27	25.3	512	50	22	2.2	0.0004	0.0002

* Total NO3 uptake rate (k_{tot}) could not be determined from tracer data

§ Denitrification rate (k_{den}) could not be determined from tracer data

Supplementary Table 2: Definitions and units of stream network model terms.

Term	Definition	Units
Q_p	discharge in stream reach p	L^3T^{-1}
ΣQ_{p-1_i}	sum of upstream contributing discharge to stream reach p	L^3T^{-1}
Q_L	discharge from the adjacent drainage area to reach p	L^3T^{-1}
Q_w	water withdrawal from reach p	L^3T^{-1}
Q_{p+1_i}	discharge to the next downstream reach, p+1	L^3T^{-1}
$NO_3^-{}_p$	nitrate in stream reach p	MT^{-1}
$\Sigma\ NO_3^-{}_{p-1_i}$	sum of upstream contributing nitrate to stream reach p	MT^{-1}
$NO_3^-{}_L$	nitrate from the adjacent drainage area to s reach p	MT^{-1}
$NO_3^-{}_R$	nitrate removal from reach p	MT^{-1}
$NO_3^-{}_{p+1_i}$	nitrate to the next downstream reach p+1	MT^{-1}
A_p	adjacent drainage area of stream reach p; the area of the catchment draining directly to stream reach p	L^2
Y_p	per unit drainage area water yield to stream reach p	$L^3L^2T^{-1}$
L_p	Per unit drainage area loading rate to stream reach p	$ML^{-2}T^{-1}$
R	proportion of $NO_3^-{}_p$ removed via biological processing	%
υ_f	vertical velocity, or mass transfer coefficient	$L\ T^{-1}$
H_L	hydraulic load; the rate of water passage through the water body relative to the benthic surface area	$L\ T^{-1}$
l	stream reach length	L
a	width coefficient	unitless
b	width exponent	unitless

Supplementary Table 3: Methods used to derive parameters used in model runs.

Term	Description of method used to derived parameters
A_p	The area draining directly to each stream reach was derived from 30-meter raster digital elevation models (USGS National Elevation Data Set, available online at http://seamless.usgs.gov) in ArcView GIS software (Version 3.3) with the Spatial Analyst extension.
Y_p	Water yield (7.69×10^{-9} m s^{-1}) was held constant across all stream reaches and model runs. The value of water yield used was the average value of calculated water yield among 106 base flow discharge measurements taken from 2nd to 6th order streams across the biomes in which the LINX II experiments were conducted. Water yield was calculated for each discharge measurement by dividing observed discharge by catchment area.
L_p	Loading rates to streams (0.001 – 100 kg km^{-2} day^{-1}) were chosen such that they reproduced the range of observed concentrations in LINX-II experimental streams. Loading rates were constant for stream reaches within each model run, but varied between model runs.
l	Stream reach length was measured from the digital hydrography dataset for the stream network as described above using ArcView GIS software (Version 3.3).
A, b	The width coefficient and exponent were derived from measured width and discharge from the same sites used to derived water yield (Y_p). Non-linear regression was performed using R-Statistical Software (Version 2.2.1, R Foundation for Statistical Computing 2005; $r^2 = 0.74$, n = 102).
v_f	The mass transfer coefficient was derived for both the constant and variable v_f scenarios. The values for v_f used in the constant scenarios were equal to the median values of observed v_f values in the LINX-II experimental streams. The variable v_f values were derived from the relationships between v_f and NO_3^- concentration (Figures. 2a and 2b in main text).

SUPPLEMENTARY FIGURES

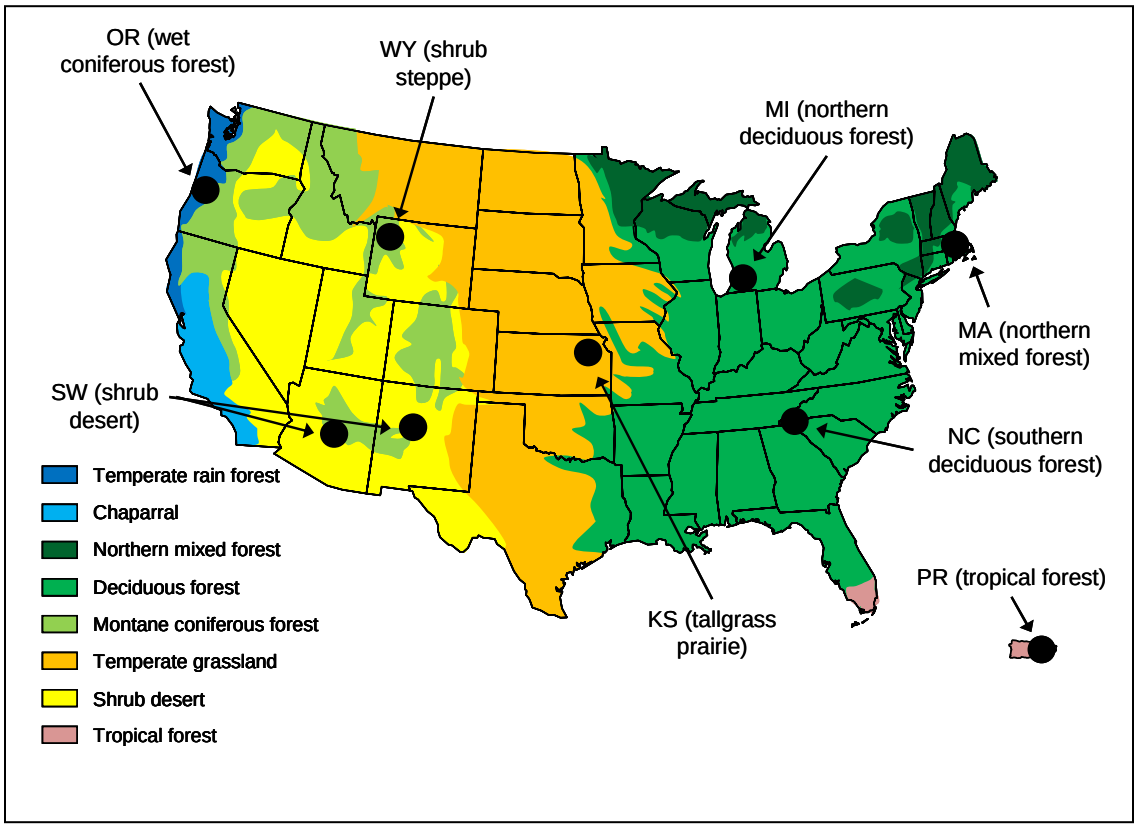

Supplementary Figure 1: Regional sites of LINX II study streams and the biomes represented. With the exception of the SW region which consisted of streams near Phoenix, Arizona, and Albuquerque, New Mexico, all streams in each region were located within about 100 km of each other (see Supplementary Table 1 for stream names and locations).

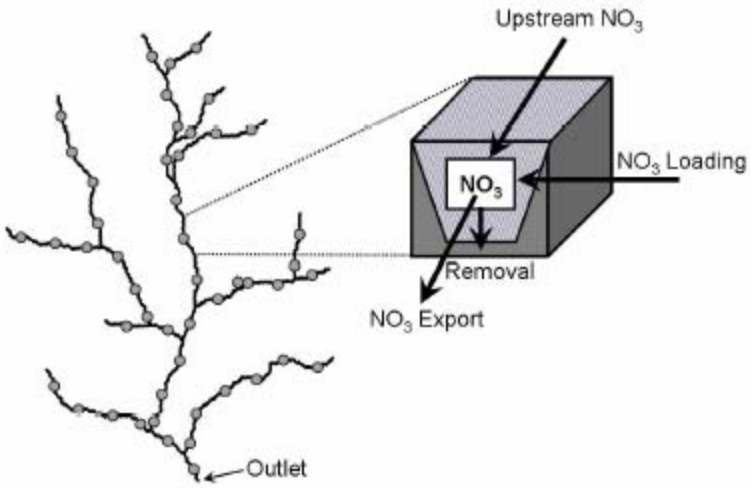

Supplementary Figure 2: An example of model structure (black lines = stream network; grey circles = model stream reaches). Stream networks are divided into segments, defined as the length of stream between tributary junctions, and segments are divided into approximately equal length reaches. For each reach, the upstream contributing reaches and the downstream receiving reach were recorded to enable the model to route flow and nitrate through the network. Within each reach, the box-and-arrow diagram represents water and nitrate flux into (upstream and loading) and out of (export and removal) the reach.

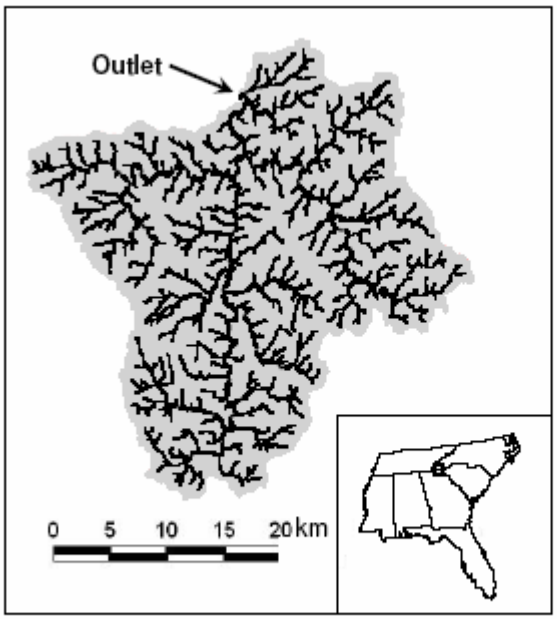

Supplementary Figure 3: The Little Tennessee River network used in the stream network model. The stream network contains 785 km of stream length and the catchment area is 821 km^2. Large and small streams as defined in Figure 4 of main text are represented as thick and thin black lines, respectively. The stream network outlet is located at 35°13'08''N and 83°22'32''W.